0013-7227/08/$15.00/0
Printed in U.S.A.

Endocrinology 149(10):4958–4969

doi: 10.1210/en.2008-0316

Alterations in RFamide-Related Peptide Expression Are Coordinated with the Preovulatory Luteinizing Hormone Surge

Erin M. Gibson, Stephanie A. Humber, Sachi Jain, Wilbur P. Williams III, Sheng Zhao, George E. Bentley, Kazuyoshi Tsutsui, and Lance J. Kriegsfeld

Departments of Psychology (E.M.G., S.A.H., S.J., W.P.W., S.Z., L.J.K.) and Integrative Biology (G.E.B.) and Helen Wills Neuroscience Institute (G.E.B., L.J.K.), University of California, Berkeley, Berkeley, California 94720; and Laboratory of Integrative Brain Sciences (K.T.), Department of Biology, Waseda University, Tokyo 169-8050, Japan

The preovulatory LH surge is triggered when the circadian pacemaker, the bilateral suprachiasmatic nucleus (SCN), stimulates the GnRH system in the presence of high estrogen concentrations (positive feedback). Importantly, during the remainder of the estrous cycle, estradiol inhibits LH release via negative feedback. We have recently documented the presence of a novel mammalian RFamide-related peptide (RFRP), a putative gonadotropin-inhibitory hormone (GnIH), that presumably acts upstream of GnRH to modulate the negative feedback effects of estrogen. The present series of studies used female Syrian hamsters to examine the possibility that, in addition to driving the LH surge positively, the SCN concomitantly coordinates the removal of steroid-mediated RFRP inhibition of the gonadotropic axis to permit the surge. We found that the SCN forms close appositions with RFRP cells, suggesting the possibility for direct temporal control of RFRP activity. During the time of the LH surge, immediate-early gene expression is reduced in RFRP cells, and this temporal regulation is estrogen dependent. To determine whether projections from the SCN regulate the timed reduction in activation of the RFRP system, we exploited the phenomenon of splitting. In split animals in which the SCN are active in antiphase, activation of the RFRP system is asymmetrical. Importantly, this asymmetry is opposite to the state of the GnRH system. Together, these findings point to novel circadian control of the RFRP system and potential participation in the circuitry controlling ovulatory function. (*Endocrinology* 149: 4958–4969, 2008)

A MASTER BIOLOGICAL pacemaker located in the suprachiasmatic nucleus (SCN) coordinates daily rhythms in behavior and physiology (1, 2). The circadian system manages daily patterns of hormone secretion required for normal health and reproductive functioning (3). Destruction of the SCN, its output, or the genes regulating cellular clock function lead to pronounced abnormalities in ovulation and fecundity (4–6). Despite the well-established role of the circadian system in regulating ovulatory function across species, the precise mechanisms by which the SCN coordinates the hormonal timing required to initiate this process remain unspecified.

The GnRH neuronal system represents the final common pathway in the neural regulation of the reproductive axis (7, 8). GnRH neurons project to the median eminence to regulate the synthesis and secretion of the pituitary gonadotropins, LH and FSH. In some species of rodents, including hamsters, the LH surge is initiated by interactions between the circadian and GnRH systems, with estrogen serving a permissive role (9). Throughout most of the ovulatory cycle, estrogen acts through negative feedback to restrain gonadotropic axis activity (10). However, during a limited time window on the day of ovulation, estrogen ceases to inhibit the reproductive axis and high estrogen concentrations are required for the initiation of the preovulatory LH surge (*i.e.* positive feedback) (11–13). This mechanism is different from that of primates, where a specific pattern of estrogen secretion is necessary to stimulate the LH surge at the level of the pituitary (14–16). In primate species, the inhibitory (negative feedback) effects of low estrogen concentrations are circumvented when estradiol rises above a threshold value and remains elevated for at least 36 h (15), with limited circadian dependence. In our rodent model system, the positive feedback effects of estrogen are contingent upon a diurnal signal from the circadian clock. In fact, a daily LH surge will occur in ovariectomized animals implanted with capsules containing estradiol levels equivalent to those found on the day of proestrus (17, 18), indicating that the coincidence of both threshold values of estrogen and a circadian signal are necessary to stimulate the release of surge levels of GnRH. In regularly cycling rodents, although the SCN is signaling the reproductive axis once daily, estradiol concentrations are permissive only on the day of proestrus. The mechanisms mediating this transient change in the effects of estrogen on the reproductive axis of rodents remain undetermined.

A great deal of research has focused on the stimulatory role of the SCN in triggering the preovulatory LH surge when estrogen levels are high (19, 20), whereas less is known regarding the neural locus on which estrogen acts to suppress

First Published Online June 19, 2008

Abbreviations: AVPV, Anteroventral periventricular nucleus; BDA, biotinylated dextran amine; DMH, dorsomedial hypothalamus; ER, estrogen receptor; GnIH, gonadotropin-inhibitory hormone; GPR147, G protein-coupled receptor 147; ir, immunoreactivity; LD, light/dark; RFRP, (Arg-Phe-NH_2)-related peptide; SCN, suprachiasmatic nucleus.

***Endocrinology* is published monthly by The Endocrine Society (http://www.endo-society.org), the foremost professional society serving the endocrine community.**

reproductive axis function during other stages of the cycle. We have recently described a novel RFamide (Arg-Phe-NH_2)-related peptide (RFRP) in rodents that putatively modulates the negative feedback effects of estrogen (21) and is orthologous to gonadotropin-inhibitory hormone (GnIH), an avian hypothalamic dodecapeptide shown to inhibit gonadotropin release (22, 23), synthesis (24), and gonadal development and maintenance (25). The RFRP gene gives rise to two biologically active peptides, RFRP-1 and RFRP-3, with administration of RFRP-3 shown to suppress LH secretion in several mammalian species, including hamsters (21, 26).

In the present series of studies, we explored the possibility that the SCN serves a dual role in ovulatory function, both applying positive drive to the GnRH system to induce the LH surge while concomitantly coordinating the removal of inhibitory influences by down-regulation of RFRP activity. We began by examining whether or not the SCN projects upon RFRP cells as a mechanism of neural control. To determine whether RFRP activity varies across the estrous cycle, we examined the activational state of the RFRP system throughout the day of proestrus and on the day of diestrus. Additionally, we used a splitting model to confirm SCN neural management over this system. Hamsters housed in a light/dark (LD) schedule exhibit one activity bout every 24 h. This activity bout is associated with symmetrical, bilateral activation of the SCN and GnRH system. When housed in constant light, some hamsters exhibit a splitting in behavior, with two daily activity bouts, each reflecting an antiphase oscillation of the left and right sides of the bilateral SCN (27–29). Notably, split animals exhibit two daily LH surges (30) and asymmetrical activation of the GnRH system (9, 27). If the RFRP system is regulated by SCN efferents and is coordinated with the LH surge, then the pattern of RFRP cell activity should also be asymmetrical and opposite to GnRH in split animals.

Materials and Methods

Animals

Adult, female LVG Syrian hamsters (*Mesocricetus auratus*) (n = 133) were used. All animals were purchased from Charles River (Wilmington, MA) at 4–5 wk of age. Animals were housed in translucent propylene cages (48 × 27 × 20 cm) and provided with *ad libitum* access to food and water for the duration of the study. Animals were maintained in a colony room at 23 ± 1 C with a 24-h LD cycle (14 h light, 10 h dark) with lights on at 0700 h and lights off at 2100 h. All experimental protocols conformed to the Institutional Animal Care and Use Committee guidelines of the University of California, Berkeley.

Tract tracing

Hamsters were deeply anesthetized with 60 mg/kg ketamine and 5 mg/kg xylazine. The head of the animal was shaved and positioned in a stereotaxic apparatus (David Kopf Instruments, Tujanga, CA), and the animal was prepared for aseptic surgery.

SCN. To examine whether or not the SCN projects to RFRP cells, small iontophoretic injections of the anterograde tracer biotinylated dextran amine (BDA) were aimed at the SCN in hamsters (n = 10). A glass micropipette (tip diameter 10–12 μm) was filled with 10% BDA (10,000 molecular weight; Molecular Probes, Eugene OR) in 0.01 M PBS (pH 7.4). Injections were aimed at the following coordinates: 0.8 mm anterior to bregma, 0.1 mm lateral to midline, and 7.9 mm below the dura. Iontophoretic injections were made using 5-mA positive current pulses (7 sec on, 7 sec off) for 7 min. Three minutes after the injection, the pipette was removed under negative current to prevent leakage of the tracer along the tract. Animals were perfused, and brains were collected 1 wk after surgery during the middle of the LD cycle (1400 h) on the day of diestrus to maximize the numbers of RFRP neurons visualized as described below.

Dorsomedial hypothalamus (DMH). To establish whether the DMH projects primarily ipsilaterally or contralaterally to hypothalamic brain sites where GnRH cells are located, pressure injections of BDA were aimed at the DMH in Syrian hamsters (n = 7). A 0.5-μl syringe (Hamilton, Reno, NV) was filled with BDA conjugated to Texas Red (1:10; Vector Laboratories, Burlingame, CA). Each animal was prepared as described above. Injections were aimed at the following coordinates: 0.5 mm posterior to bregma, 0.4 mm lateral to midline, and 8.3 mm below the dura. Over a 10-min period, 300 nl BDA was injected. One week after stereotaxic surgery, animals were perfused and brains were collected as described below.

Serum collection

Animals were anesthetized using isoflurane, and blood samples were collected from the retroorbital sinus. Samples were collected at 1300, 1600, 1700, 1800, 1900, 2000, and 2300 h (n = 8 per time point) on the day of the LH surge and 1300 h on the day before the surge (*i.e.* diestrus).

Examination of RFRP cellular activity around the time of the LH surge

Estrous cyclicity was monitored by daily examination of vaginal discharge from all hamsters. There is a reliable release of discharge every 4 d, on the day of proestrus (31). Animals were monitored for at least 3 wk for estrus regularity. Only hamsters with regular, 4-d estrous cycles were used. The day on which vaginal discharge was observed was designated as the day of proestrus. Brains were collected at 1300, 1600, 1700, 1800, 1900, 2000, and 2300 h (n = 8 per time point) on the day of the LH surge. One additional group was examined at 1300 h on the day before the LH surge (*i.e.* diestrus) to examine the state of RFRP cell activation when LH is maximally inhibited by estrogen feedback.

Examination of the role of estrogen in RFRP control

Because estrogen concentrations are elevated for an extended period on the day of proestrus, it is possible that any changes in RFRP expression require the presence of this sex steroid. To determine whether inhibitory RFRP cells require estrogen to alter their activity during the LH surge, additional groups of animals were bilaterally ovariectomized (n = 16) under isoflurane anesthetic. Subsequently, animals were either implanted with a SILASTIC brand capsule (Dow Corning Corp., Midland, MI; 10-mm length, 1.45-mm inner diameter, 1.93-mm outer diameter) containing powdered 17-estradiol (n = 8) or an empty capsule (n = 8). In estrogen-implanted animals, this treatment provides estradiol concentrations comparable to those seen on the day of proestrus (32) and results in daily LH surges at the same time of day that the LH surge would normally occur (33). Animals were perfused as described below just before the LH surge (2000 h) or after the surge (2300 h).

Examination of RFRP receptor expression in the pituitary

Because a significant number of GnRH cells receive RFRP input across species (34), the present study was principally concerned with gonadotropin regulation via this mechanism. However, reports in other species indicate actions of RFRP at the level of the pituitary (35, 36). As a result, we examined whether or not RFRP receptor expression is seen in the pituitary of female Syrian hamsters, as a potential additional mechanism of regulatory control using RT-PCR. Pituitaries from Syrian hamsters (n = 2) were examined, whereas liver tissue from rat (n = 1) was used as a negative control (37). Tissue was collected, its total RNA was extracted (RNeasy Mini Kit; QIAGEN Inc., Valencia, CA), and 3′-RACE cDNA was then synthesized (SMART cDNA synthesis kit; Clontech Laboratories Inc., Palo Alto, CA). Touchdown PCR was conducted using specific primers for hamster G protein-coupled receptor 147 (GPR147),

the cognate receptor for RFRP (sense, TCTCG GGCCA GGCCT CCCAG CA, and antisense, TCTCG GGCCA GGCCT CCCAG CA). Initial denaturing occurred for 3 min at 95 C followed by 16 touchdown cycles from 68 C to 60 C (annealing temperature, decreased 0.5 C every cycle) and continued for another 25 cycles with 60 C annealing temperature. PCR products were detected on a 1% agarose gel.

Splitting induction

After 1 wk in a 14-h light, 10-h dark cycle (lights on 0700 h), an additional group of Syrian hamsters (n = 30) was transferred to constant light (LL) conditions. Wheel running activity was recorded continuously using VitalView (MiniMitter Co., Inc., Sunriver, OR) for 12 wk. Accumulated counts were rescored every 10 min and stored to the attached computer. After 8 wk of exposure to constant light, animals were ovariectomized and sc implanted with a SILASTIC brand capsule (10-mm length, 1.45-mm inner diameter, 1.93-mm outer diameter) filled with powdered 17-estradiol (Sigma Chemical Co., St. Louis, MO). Animals were perfused as described below less than 1 h before one activity bout in split animals (n = 9) and either 1 h (n = 6) or 13 h (n = 5) before the activity bout in nonsplit animals. Ten animals did not exhibit regular activity patterns and were not used in this study.

Perfusion and histology

Tract tracing. Hamsters were deeply anesthetized with sodium pentobarbital (200 mg/kg) and perfused intracardially with 150 ml 0.9% saline, followed by 300–400 ml 4% paraformaldehyde in 0.1 M PBS (pH 7.4). Brains were postfixed for 2–3 h at 4 C and cryoprotected in 30% sucrose in 0.1 M PBS overnight. For visualization of SCN injected with BDA and RFRP, every fourth 35-μm coronal section was washed in PBS, incubated in 1% H_2O_2, and then incubated in 0.4% Triton X-100 (PBT) for 1 h. Sections were then incubated in avidin-biotin complex (ABC Elite Kit; Vector; 1:1000 in PBT) for 1 h at room temperature. To amplify the BDA signal, sections were then incubated in biotinylated tyramide (0.6%) for 30 min at room temperature before incubation in CY-2-conjugated streptavidin (1:200) for 60 min. After labeling for BDA, sections were labeled using an antibody directed against RFRP (1:10,000; Pacific Immunology 123/124) as previously described and validated (21) with CY-3 donkey antirabbit (1:200; Jackson ImmunoResearch, West Grove, PA) as the secondary antibody/fluorophore. For visualization of BDA in the DMH, the above procedure was followed but BDA was visualized using CY-3 conjugated streptavidin (1:200; Jackson ImmunoResearch) and RFRP was visualized using CY-2 donkey antirabbit (1:200; Jackson ImmunoResearch).

RFRP and GnRH cellular activity. For simultaneous visualization of RFRP and FOS across the estrous cycle, every fourth 40-μm coronal section from the mediobasal hypothalamus was washed in 0.1 M PBS, incubated in 0.5% H_2O_2, and incubated in normal goat serum (1:50; Jackson ImmunoResearch) in 0.1% Triton X-100 (PBT) for 1 h. Sections were then incubated for 48 h at 4 C with a rabbit anti-FOS antibody diluted at 1:50,000 (Santa Cruz Biotechnology, Santa Cruz, CA) and normal goat serum diluted at 1:1000 with 0.1% PBT for 48 h. After incubation in anti-FOS, brains were incubated for 1 h in biotinylated goat antirabbit (1:300; Vector) and then in avidin-biotin complex for 1 h. The FOS signal was amplified with biotinylated tyramide solution (0.6%) for 30 min as previously described (21). Cells were then labeled by using CY-2-conjugated streptavidin (1:200; Jackson ImmunoResearch) as the fluorophore. This protocol allowed for the amplification of the highly diluted anti-FOS required for double labeling with two antibodies generated in the same species (rabbit). After labeling for FOS, sections were incubated in anti-RFRP antibody (1:10,000; PAC 123/124) in 0.1% PBT for 48 h (21). RFRP cells were labeled with CY-3 donkey antirabbit (1:200; Jackson ImmunoResearch) as the secondary antibody/fluorophore. For simultaneous visualization of RFRP and FOS in split animals (and their unsplit controls), this same procedure was applied using an anti-RFRP antibody directed against the Syrian hamster form of this peptide (1:10,000; PAC 1365). Double-label immunohistochemical studies using PAC 123/124 and PAC 1365 confirmed that these two antibodies label the same population of cells in the DMH. The prior double-labeling protocol without the addition of the RFRP primary antibody was performed to control for the possibility of two primary antibodies generated in the same species cross-reacting. This control confirmed the specificity of this procedure with robust FOS expression and the absence of signal when excited using the standard wavelength for CY-3.

The previous FOS/RFRP protocol was followed for visualization of GnRH and FOS with the RFRP antibody replaced with an antibody directed against GnRH (mouse; 1:2000; Abcam, Cambridge, MA). Cells were visualized using CY-3 donkey antimouse (1:200; Jackson ImmunoResearch). All sections immunohistochemically treated were

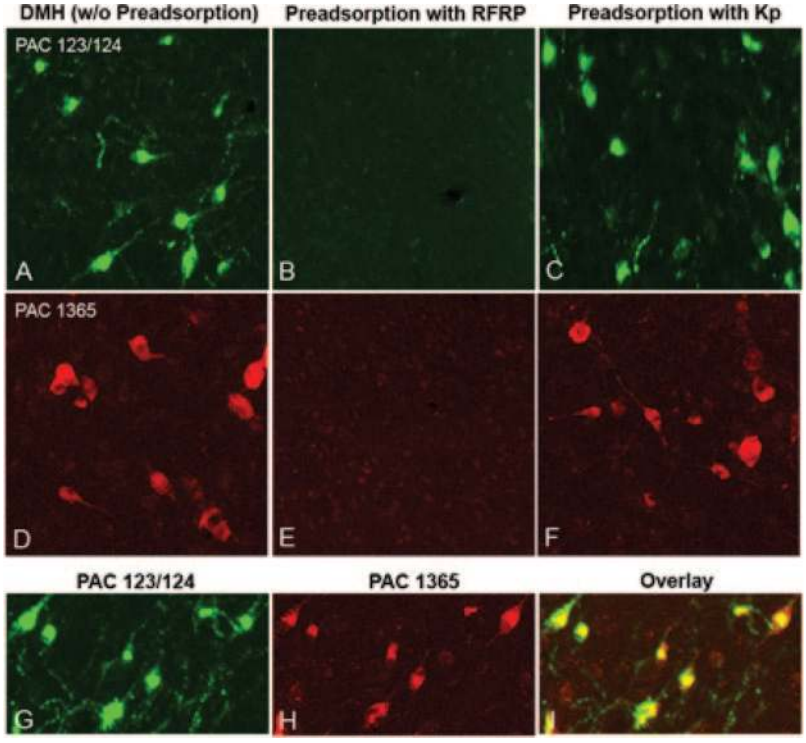

FIG. 1. RFRP-ir labeling is abolished with hamster RFRP peptide preadsorption. Photomicrographs of RFRP-ir cell body labeling in the DMH using PAC 123/124 (A) and PAC 1365 (D). Preadsorption with hamster RFRP peptide (B and E) abolishes RFRP staining. Staining of RFRP is not affected by preadsorption with kisspeptin peptide (Kp, C and F). RFRP antibodies PAC 123/124 (G) and PAC 1365 (H) label the same cell populations (I).

mounted onto gelatin-coated slides and dehydrated in a graded series of alcohols, and coverslips were applied.

SCN cellular activity. To identify split and nonsplit SCN, FOS activation in the SCN was visualized fluorescently using an antibody directed against FOS as described above and with 3,3′-diaminobenzidine (Vector). Sections were mounted, dehydrated, and coverslipped as described previously.

Control procedures. Several control procedures were implemented to ensure the specificity of immunohistochemical labeling. PAC123/124 RFRP antibody raised against the white-crowned sparrow form of the peptide was preadsorbed with avian and rat RFRP ligand for 24 h before tissue application as described previously (21) and was shown to eliminate staining. Additional controls with PAC 123/124 and PAC 1365, raised against the Syrian hamster form of the peptide, preadsorbed with Syrian RFRP ligand, were performed. This procedure eliminated staining in both cases (Fig. 1, B and E). Because kisspeptin is an RFamide peptide with a C-terminal structure similar to that of RFRP, RFRP antibodies (both PAC 123/124 and PAC 1365) were preadsorbed with kisspeptin peptide to examine potential cross-reactivity. This procedure did not result in a change in the pattern or intensity of RFRP cell body labeling, indicating that the antibody does not exhibit cross-reactivity with this peptide (Fig. 1, C and F). Finally, double-label studies with PAC123/124 and PAC1365 confirm that both antibodies label identical cell populations (Fig. 1, G–I). Previously, a competitive ELISA was used to confirm the specificity of PAC 123/124 RFRP antibody. Cross-reactivity was not observed for any of the closely related peptides (carp, mollusk, bovine, or chicken RFamide) (22). Additional studies using a competitive ELISA were recently conducted indicating the absence of cross-reactivity with LPLRFa, neuropeptide FF (NPFF), prolactin-releasing peptide (PrRP), and FMRFamide peptides (Bentley, G. E., and K. Tsutsui, unpublished observations).

Light microscopy

Sections were investigated using a Zeiss Z1 microscope (Carl Zeiss, Thornwood, NY). Sections were examined using the standard wavelengths for CY-2 (488 nm) and CY-3 (568 nm). Every fourth section through the DMH, or 12 sections per animal, and the medial preoptic area, or 10 sections per animal, were assessed, and those areas expressing RFRP immunoreactivity (RFRP-ir) and GnRH-ir were investigated for coexpression with FOS protein using confocal microscopy (see below). For light microscopy, areas identified as having double-labeled cells were digitally captured at ×200 in 8-bit greyscale using a cooled CCD camera (Zeiss). Each label was captured as a single image without moving the position of the stage or plane of focus between captures. Images were superimposed digitally. Brain areas were examined for double labeling using Photoshop software in which CY-2 and CY-3 channels could be turned on and off independently. Only those RFRP and GnRH cells with a visible nucleus in which FOS expression was localized were counted as double-labeled cells. The total numbers of

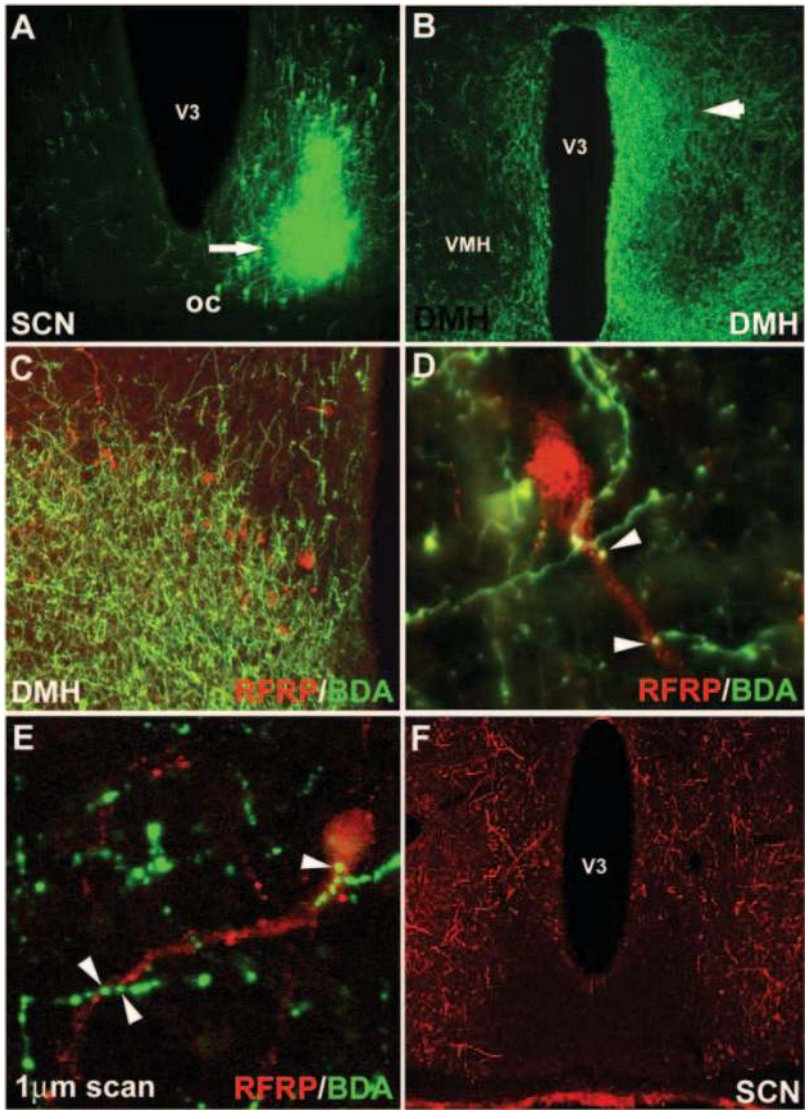

FIG. 2. SCN fibers project to RFRP-ir cells in the DMH. A, Example injection site from an injection of BDA that filled the ventrolateral aspect of the SCN; B, low-power photomicrograph indicating terminal fibers from the SCN project to the DMH, principally ipsilaterally; C–E, examples of SCN projections in close apposition to RFRP-ir cells in the DMH at the light (C, low power; D, high power) and confocal levels (E); F, RFRP fibers target the sub-paraventricular zone and retrochiasmatic area but do not terminate in the SCN. V3, Third ventricle.

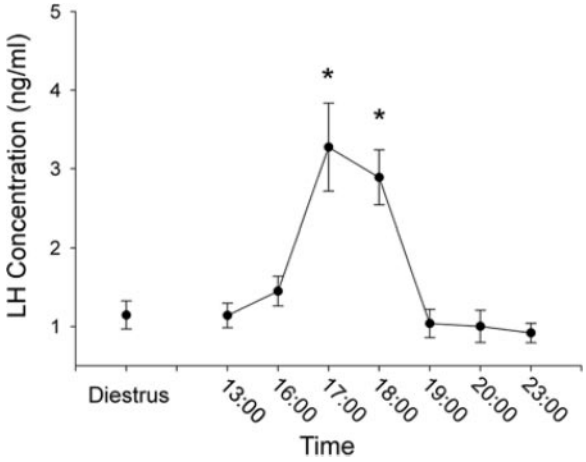

FIG. 3. LH concentrations in Syrian hamsters. Mean (±SEM) LH concentrations on the day of diestrus and during various times on the day of proestrus. *, Significantly different from diestrous values and all other proestrous values, excluding 1600 h, $P < 0.05$.

RFRP cells and GnRH cells and the percentage of cells expressing FOS were recorded by two independent observers blind to the experimental conditions.

Confocal microscopy

Brain sections used for light microscopy were also used for the confocal scans to confirm results at the conventional microscopy level. RFRP cells with putative SCN contacts were scanned through the extent of each cell in 0.5-μm increments. Only those cells in which the BDA-labeled fiber contacted an RFRP cell in the same 0.5-μm scan were counted as close contacts. Cells characterized as being double labeled with FOS/RFRP or FOS/GnRH at the conventional microscopy level were confirmed in the same manner to ensure that FOS was expressed within the cells rather than in overlapping cells in the same field of view. Likewise, cells classified as single labeled were assessed to ensure that the conventional microscopy strategy did not result in false negatives. At least 10% of those cells quantified using conventional microscopy were assessed in confocal scans. The cells assessed using confocal microscopy were chosen randomly across groups. Regions of the brain with putative double labels identified at the light level were scanned at ×400 using confocal microscopy. Cells were observed under a Zeiss Axiovert 100TV fluorescence microscope with a Zeiss LSM 510 laser scanning confocal attachment. The sections were excited with an argon-krypton laser using the standard excitation wavelengths for CY-2 and CY-3. Stacked images were collected as 1.0-μm multitract optical sections. Using the LSM 3.95 software (Zeiss), red and green images of the sections were superimposed. RFRP or GnRH cells in a given brain region were examined through their entirety in 1.0-μm steps. Captured images were examined for double labeling using Photoshop.

LH RIAs

Serum LH concentrations were measured in duplicate in a single RIA with reagents obtained from the National Institutes of Health (Bethesda, MD) as previously described (38). The antiserum was rLH-S-11, and the standard was rLH-RP3. The sensitivity was 0.01 ng/tube, and the intraassay coefficient of variation was 2.8% for the low pool and 8.4% for the high pool. The antisera were highly specific for the hormones measured, with low cross-reactivity with other hormones.

Statistics

Data for RFRP cell counts, FOS expression in RFRP cells, and LH results were analyzed using one-way ANOVA for those studies relating to the

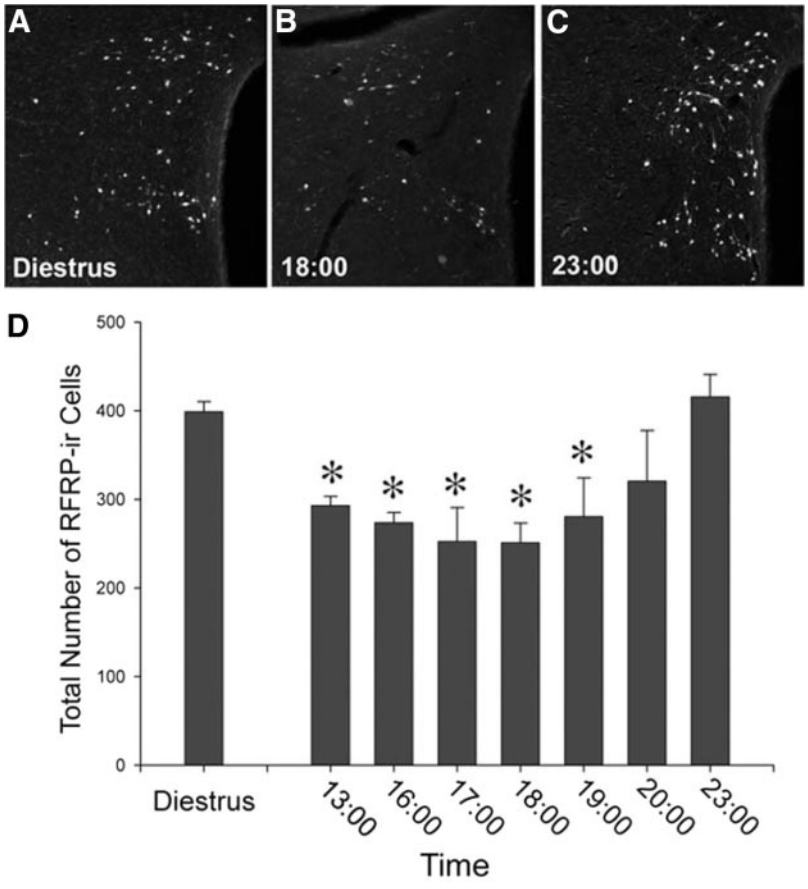

FIG. 4. RFRP-ir cell numbers are reduced during the LH surge and reinstated thereafter. A, Low-power photomicrograph of RFRP-ir cell body labeling in the DMH on the day of diestrus; B and C, low-power photomicrographs of RFRP-ir cell body labeling in the DMH on the day of proestrus during the trough (1800 h) and peak (2300 h) of expression, respectively; D, mean (±SEM) RFRP-ir cell counts on the day of diestrus and throughout the day of proestrus. *, Significantly different from diestrous values and 2300-h values on the day of proestrus, $P < 0.05$.

change in activation over the estrous cycle. Total cell counts and FOS expression in RFRP and GnRH cells in split and nonsplit (NS) animals were analyzed using two-way analyses of variance: condition (split or NS) × lateralization. Group differences were evaluated using Tukey tests when sample sizes were equal and Tukey-Kramer tests when sample sizes were unequal (*e.g.* split data). Differences were considered significant if $P < 0.05$.

Results

The SCN projects extensively to RFRP-ir cells in the DMH

Of the 10 hamsters injected with BDA, five injections were localized to the SCN and five misses were centered in the adjacent hypothalamus and retrochiasmatic area. Three injections filled the SCN unilaterally, whereas one injection was centered in the dorsomedial SCN and another in the ventrolateral SCN (Fig. 2A). All five injections resulted in extensive projections and terminal fields in the DMH (Fig. 2B). These smaller, localized injections in the SCN provided the opportunity to investigate the subregions from which identified projections originate. As in our previous work (21), RFRP-ir cells were confined to the DMH (Fig. 2C). For the three whole SCN injections, contacts upon RFRP perikarya ranged from 56.4–65.2% (Fig. 2, D and E). A dorsomedial injection resulted in 20.4% of RFRP cells receiving SCN contacts, whereas 48.3% of RFRP cells were labeled with a comparably sized ventrolateral injection. Despite marked projections from the SCN to the RFRP system, RFRP cells did not project back to the SCN at any time point investigated (Fig. 2F). In all cases, RFRP fiber labeling was absent in the SCN, with dense projections targeting the adjacent sub-paraventricular zone and retrochiasmatic area (21).

RFRP-ir cell numbers are reduced during the LH surge and reinstated thereafter

All females exhibited regular 4-d estrous cycles. The preovulatory LH surge began at 1700 h on the day of proestrus and was complete within 2 h (Fig. 3). On the day of diestrus II, RFRP cell numbers were maximal in the DMH. In Syrian hamsters held in a 14-h light, 12-h dark cycle, LH concentrations peak 4 h before lights out on the day of proestrus, with an initial increase seen 6 h before dark and cessation of the surge about 2 h before darkness (39). On the day of proestrus, RFRP-ir cell numbers were reduced relative to the day of diestrus II for all time points ($P < 0.05$ in each case) excluding 2000 and 2300 h ($P > 0.05$ in each case) (Fig. 4). In all cases, quantification of FOS-positive RFRP-ir and FOS-negative RFRP-ir cells at the confocal level agreed with assessment at the conventional microscopy level.

Activational state of RFRP cells is reduced during the LH surge and reinstated thereafter

As with RFRP cell numbers, the percentage of RFRP-ir cells expressing FOS was greatest during diestrus II when estrogen is maximally inhibiting LH production ($P < 0.05$ relative to all other time points). Relative to diestrus II, on the day of proestrus, RFRP cell activity was reduced at all time points

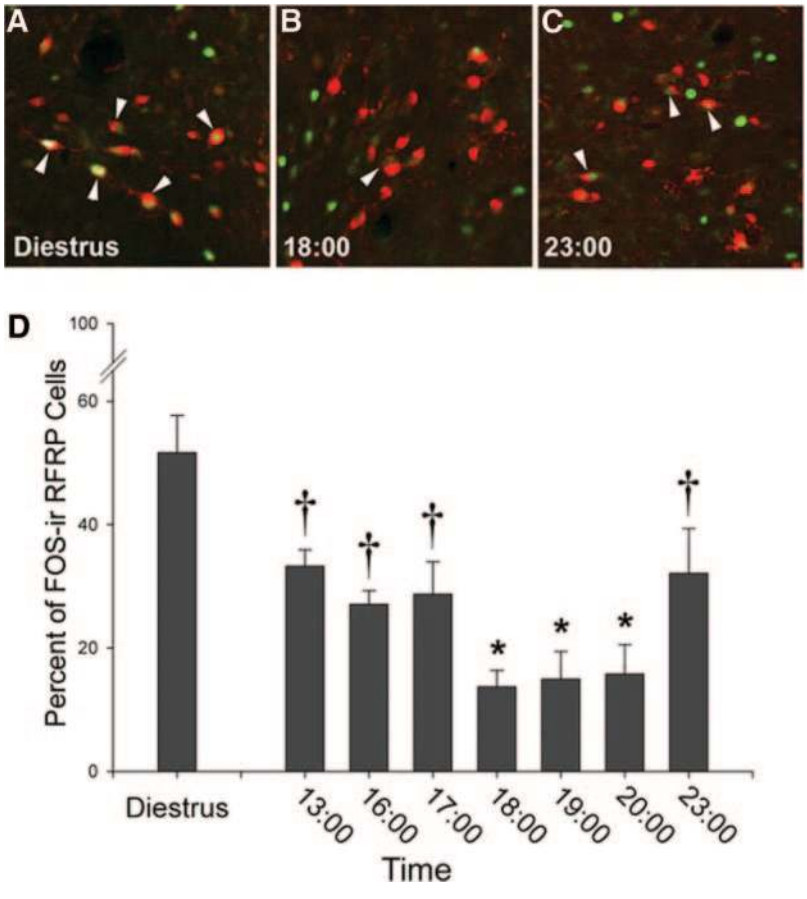

FIG. 5. Activation of RFRP-ir cells is reduced during the LH surge and reinstated thereafter. The percentage of RFRP-ir cells expressing FOS is reduced on the day of proestrus, around the time of the LH surge. A–C, Low-power photomicrographs of RFRP-ir cells expressing FOS on the day of diestrus (A) and during the trough (B) and peak (C) of expression on the day of proestrus. D, Mean (±SEM) percentage of RFRP-ir cells expressing FOS on the day of diestrus and throughout the day of proestrus. All *bars* not sharing a *symbol* differ significantly from each other at $P < 0.05$.

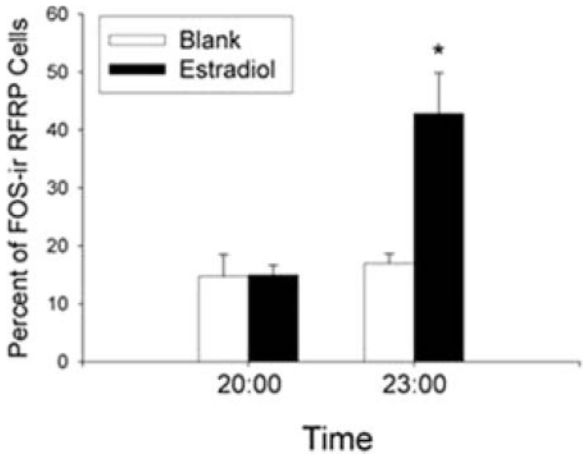

FIG. 6. Estrogen is required for daily changes in activational state of RFRP-ir cells. Shown is the mean (±SEM) percentage of RFRP-ir cells expressing FOS in ovariectomized hamsters implanted with estradiol or a blank capsule during the LH surge (2000 h) or after the LH surge (2300 h). *, Significantly different from all other values, $P < 0.05$.

($P < 0.05$; Fig. 5). Importantly, maximal reductions in FOS expression are observed 3 h before lights out, with sustained reductions in activity until 2000 h ($P < 0.05$; Fig. 5). Generally, FOS expression represents cellular activity about 1 h before killing (40), suggesting that maximal reductions in RFRP cellular activity occurred between 4 and 2 h before lights out. After the time of the LH surge in hamsters (2300 h), RFRP cellular activity was increased ($P < 0.05$; Fig. 5). In all cases, quantification of FOS-positive RFRP-ir and FOS-negative RFRP-ir cells at the confocal level agreed with assessment at the conventional microscopy level.

Daily changes in RFRP cellular activity require estrogen

Because estradiol levels are maximal on the day of proestrus, we examined whether changes in the state of RFRP cells require the presence of this hormone. Based on the results above, we examined estradiol-treated and control hamsters at 2000 h (low RFRP cellular activity on the day of proestrus) and 2300 h (high RFRP activity). Estradiol-implanted hamsters exhibited low RFRP cell FOS expression at 2000 h with a marked increase at 2300 h ($P < 0.05$). In contrast, hamsters without estradiol replacement had low RFRP cell FOS expression at both time points ($P > 0.05$; Fig. 6). In all cases, quantification of FOS-positive RFRP-ir and FOS-negative RFRP-ir cells at the confocal level agreed with assessment at the conventional microscopy level.

The DMH projects ipsilaterally to hypothalamic regions containing GnRH cells

Of the seven hamsters injected with BDA, three were localized to the DMH. For all three injections, projections from the DMH to all forebrain and hypothalamic sites expressing GnRH neurons, including the tenia tectum, medial and lateral septum, diagonal band of Broca, preoptic area, and anterior hypothalamus, were principally ipsilateral (for preoptic area, see Fig. 7).

RFRP activity is lateralized and associated with the LH surge in split hamsters

When held in constant light, 11 hamsters maintained one bout of activity, whereas nine animals split their activity into two antiphase bouts (Fig. 8, A and B). In nonsplit controls, as expected, GnRH neurons exhibited maximal FOS expression 1 h (NS1) before their activity bout compared with animals killed 13 h (NS13) before activity ($P < 0.05$; Fig. 8, C and E); activity was symmetrical for both hemispheres ($P > 0.05$). In contrast, RFRP cell activity showed the opposite pattern, with minimal expression in NS1 hamsters compared with NS13 animals ($P < 0.05$; Fig. 8, G and I). When hamsters with split behavior were examined, GnRH FOS expression was asymmetrical, with maximal activity on the side of the brain ipsilateral to the activated SCN ($P > 0.05$; Fig. 8, D and F). The opposing pattern of activity was seen in the RFRP system, with higher FOS expression in RFRP cells contralateral to the activated SCN ($P < 0.05$; Fig. 8, H and J). In all cases, quantification of FOS-positive RFRP/GnRH-ir and FOS-negative RFRP/GnRH-ir cells at the confocal level agreed with assessment at the conventional microscopy level.

RFRP cells project to the median eminence, and hamster pituitary expresses RFRP receptors

RFRP-ir cells in the DMH project extensively to the median eminence in hamster tissue, indicating RFRP may mediate the LH surge at the level of the median eminence and pituitary (Fig. 9B). Using RT-PCR, we investigated the existence of RFRP receptor in the pituitary of Syrian hamsters by examining pituitaries from two different hamsters as well as liver tissue from rat as a control, which has previously been shown not to express RFRP receptors (37). As expected, pituitary tissue exhibited

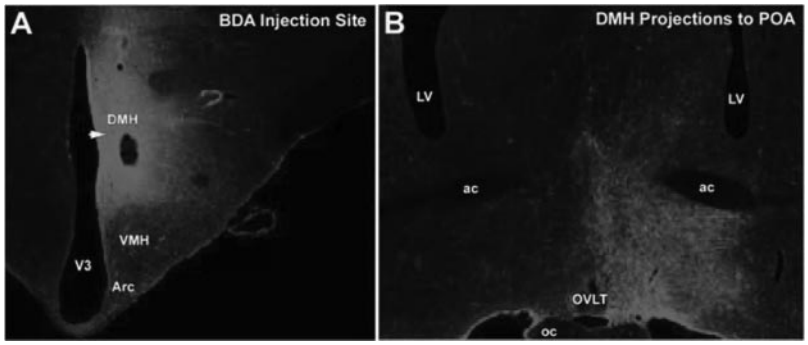

FIG. 7. The DMH projects ipsilaterally to hypothalamic regions containing GnRH-ir cells. A, Representative injection of the anterograde tracer, BDA, localized to the DMH; B, DMH projections were localized to numerous hypothalamic regions containing GnRH-ir cells, including the preoptic area. Projections were principally ipsilateral. ac, Anterior commissure; Arc, arcuate nucleus; LV, lateral ventricle; oc, optic chiasm; OVLT, organum vasculosum of the lamina terminalis, V3, third ventricle; VMH, ventromedial hypothalamus.

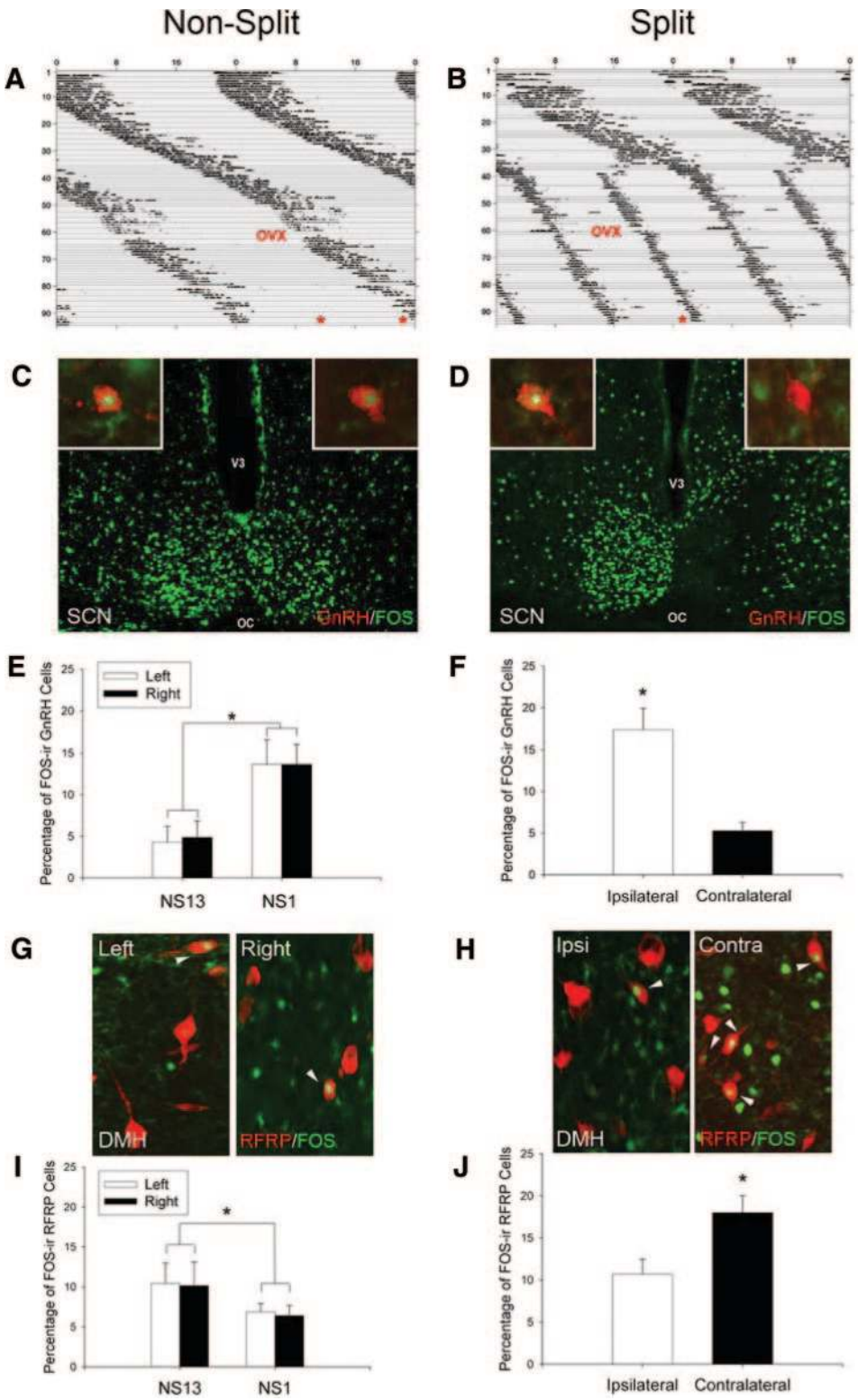

FIG. 8. Lateralization of GnRH and RFRP activational patterns in split hamsters is associated with the LH surge. A and B, Actograms of wheel-running activity in estradiol-implanted, ovariectomized (OVX) hamsters kept in constant light conditions (LL). A, Nonsplit (NS) hamsters were killed (*) 1 or 13 h before the onset of the activity bout. B, Split hamsters were killed (*) 1 h before the onset of one of the two activity bouts. C and D, Photomicrographs of FOS activation in SCN and GnRH cells (*insets*) of NS and split hamsters. E and F, Mean (±SEM) percentage of FOS-ir GnRH cells in nonsplit hamsters killed 1 h (NS1) or 13 h (before the surge; NS13) before their activity bout and split hamsters killed 1 h before one of their activity bouts. G and H, Photomicrographs of FOS-ir RFRP cells in the DMH of NS and split hamsters. I and J, Mean (±SEM) percentage of FOS-ir RFRP cells in NS1, NS13, and split hamsters. *, Significantly different from all other values, $P < 0.05$. oc, Optic chiasm; V3, third ventricle.

robust expression of RFRP receptors, whereas rat liver tissue and a control sample did not express RFRP receptors (Fig. 9A).

Discussion

A host of neurochemicals suppresses GnRH secretion, with the inhibitory transmitters γ-aminobutyric acid (41–43) and the endogenous opioids (44–46) receiving the most attention. However, a mechanism coordinating disinhibition from these suppressive factors during stimulation of the LH surge of the estrous cycle has not been identified. Here we show a novel neural locus and neuropeptidergic system that displays properties consistent with such a role. The present

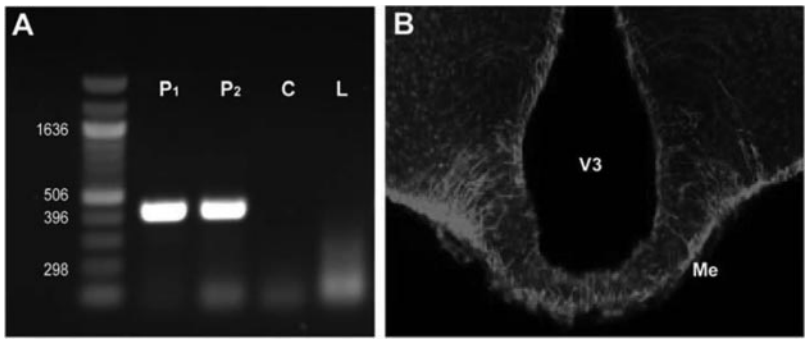

FIG. 9. Hamster pituitary expresses RFRP receptors, and RFRP-ir cells project to median eminence. A, Using RT-PCR, pituitaries from two hamsters (P1 and P2) were shown to express the RFRP receptor, GPR147. RFRP receptor expression was not detected in a control sample (C), water, or in tissue from rat liver (L) that was previously shown not to express RFRP receptors (37). B, RFRP fibers from the DMH project to the median eminence (Me), suggesting control of the LH surge may also occur at the level of the median eminence and the pituitary. V3, Third ventricle.

findings point to interactions between the circadian and RFRP systems in the control of the preovulatory LH surge. Anterograde tracing shows pronounced projections from the SCN to the RFRP neuronal system, with close contacts of presumptive SCN terminals on RFRP cell perikarya. The RFRP system exhibits reduced expression and activity on the day of proestrus, with activity markedly suppressed around the time window in which the LH surge occurs. These findings suggest alterations in RFRP peptide synthesis, secretion, and/or transport throughout the ovulatory cycle. The system returns to presurge activity levels during early evening on the day of ovulation, after the surge has ceased. Additionally, we observed an asymmetry in the activational state of the RFRP system at the time of the surge that was opposite to the state of the GnRH system in split animals. Together, these findings suggest a novel network of ovulatory control with the possibility that the circadian system serves a dual role, both stimulating GnRH cell activity to initiate the LH surge as well as coordinating disinhibition from the influences of estrogen.

At the time of ovulation, GnRH neurons exhibit a robust increase in immediate-early gene expression, with activation lagging behind the initiation of the LH surge by about 1 h (47–51). In ovariectomized Syrian hamsters held in a 14-h light, 10-h dark cycle, LH concentrations peak 4 h before lights out on the day of proestrus, with cessation of the surge about 2 h before darkness (39) (present study, Fig. 3). The present findings indicate a pattern of FOS expression in RFRP cells opposite to that observed for GnRH, further suggesting complementary circadian control of both systems. The SCN projects extensively to RFRP-ir cells, with both dorsomedial and ventrolateral subregions of the SCN projecting to the DMH. Whereas only one animal was assessed for anterograde injections into both subregions of the SCN, these results provide a possible avenue for future investigation of SCN control of the RFRP system. At the conventional and confocal microscope levels, we observe close appositions between SCN terminals and RFRP cells. Although laser scanning confocal microscopy is not adequate to identify true synapses onto RFRP neurons, high-power confocal scans showing a presumptive bouton contacting a cell body in the same optical plane provide strong support for a functional relationship between the fiber and the cell body it is contacting.

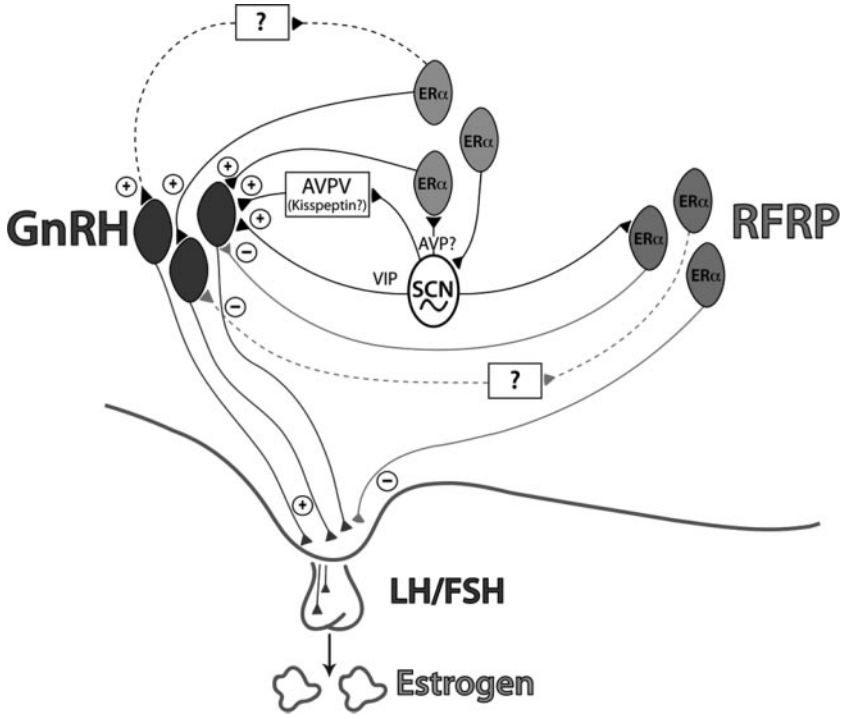

FIG. 10. Integration of RFRP in regulating induction of the LH surge. A proposed model incorporating a role for the RFRP system in the ovulatory circuitry. *Dark black lines* depict projections from the circadian system to GnRH neurons and neurons containing ERs (61) as well as to the RFRP system (present study) and the AVPV (57) reported in rats, mice, and hamsters. Kisspeptin cells in the AVPV are active at the time of the LH surge (62, 63). Neurons containing ER-α in the preoptic area and elsewhere are known to project to the SCN (58) and to GnRH neurons (64) and may play a role in mediating the circadian signal to GnRH neurons directly and/or indirectly. *Light solid lines* depict interactions between the RFRP and GnRH systems described in the present study and our previous work (21). These *lines* indicate a putative role for RFRP in modulating the negative feedback effects of estrogen (21), with SCN communication allowing for removal of negative feedback on the reproductive axis during the time of the LH surge. *Dashed lines* indicate indirect connections between systems that have not yet been explored. According to the model generated from the present findings, RFRP cells respond to estradiol with hypothalamo-pituitary-gonadal axis inhibition during most of the estrous cycle. At the time of the LH surge, however, the SCN signals the RFRP system to ignore estradiol input and remove negative feedback influences on the hypothalamic-pituitary-gonadal axis, allowing activation of the GnRH system directly or indirectly via the circadian system. AVP, Arginine vasopressin; VIP, vasoactive intestinal polypeptide.

Our analysis of split animals suggests neural circadian control of the RFRP system. RFRP cells exhibit reduced activity on the side of the brain bearing the activated SCN, a pattern opposite to GnRH cell activation (Fig. 8). These findings, along with anterograde tracing results showing that the DMH projects to ipsilateral brain regions containing GnRH cells, are consistent with the notion that the SCN coordinates disinhibition of the RFRP system with the initiation of the surge (Figs. 7 and 10). Overall, FOS expression in RFRP-ir cells in split and nonsplit animals was reduced relative to animals housed in a LD cycle. This finding is likely due to constant light conditions, because a similar reduction has been observed previously under these conditions (9). It remains possible that the RFRP system also modulates the surge at the level of the pituitary, because the RFRP receptor, GPR147 (35, 37, 52), is present in hamster (present study) and quail (25) pituitary, with RFRP fibers extending into the median eminence (25) (Figs. 9 and 10). We previously reported sparse RFRP fibers extending into the external layer of the median eminence (21), but refinements of our amplified immunohistochemical procedures in the present report indicate more pronounced innervation than previously suggested, in agreement with reports in other species.

In rats, mice, and hamsters, RFRP cells project to GnRH cells directly, providing a potential pathway for its suppressive actions (21). Likewise, in avian species, RFRP cells also project to GnRH cells (34, 65), and GnRH neurons express GnIH, the RFRP ortholog found in birds, receptor mRNA (65). Although the pattern of transcriptional activation of RFRP cells is consistent with a release of the reproductive axis from RFRP inhibition at the time of the surge, it is possible that RFRP cellular activity is unrelated to timed changes in reproductive axis activity. RFRP cells project widely in mammalian brain throughout midline hypothalamic regions and limbic structures, suggesting actions in addition to GnRH control (21). However, recent observations indicate that injections of RFRP-3 inhibit GnRH neuronal activation during the estradiol-induced LH surge (53), suggesting a need for the removal of RFRP influences at this time. Whether such removal of RFRP inhibition to the reproductive axis occurs normally during ovulation requires further study.

RFRP-ir cells exhibit changes in FOS expression on the day of proestrus, when estrogen concentrations are chronically elevated. Given the design of the present series of experiments, we cannot discern the specific contribution of the circadian system *vs.* stage of cycle (*i.e.* proestrus) to changes in RFRP cell FOS expression. Several lines of evidence point to a role for both factors in this daily regulation. First, when estrogen concentrations are clamped at proestrous levels, the RFRP system exhibits the same timed pattern of activation, with timed changes abolished in ovariectomized animals given empty implants (Fig. 6). Additionally, the abolition of this daily pattern in RFRP activity in animals implanted with empty capsules suggests a circadian mechanism requiring estrogen. Further studies examining the daily pattern of RFRP cellular function during other stages of the cycle are necessary to fully explore this possibility. Collectively, these findings suggest the possibility that RFRP cells exhibit daily changes in responsiveness to estrogen, with reduced sensitivity around the time of the LH surge. Alternatively, because only a subset of these cells express estrogen receptor (ER)-α (21), it is possible that cells expressing temporal changes in activity are not estrogen responsive but, instead, are controlled by an estrogen-responsive clock mechanism. Whether estrogen acts upstream of RFRP cells to modulate their activity remains to be determined.

Whereas circadian behavior, such as wheel running, can be supported via diffusible signals (54), all findings to date indicate that neural communication from the SCN is required for initiation of the LH surge (3, 5, 9, 32, 55). In addition to direct connections to GnRH neurons, the SCN projects extensively to the anteroventral periventricular nucleus (AVPV), a brain region associated with the induction of the preovulatory LH surge and changes in progesterone receptor expression (11, 56). The role of progesterone in the regulation of the RFRP system is unknown and may provide insight into an additional mechanism of ovulatory control. The cells to which the SCN projects are estrogen responsive (57), suggesting that the AVPV may be an important integration point for circadian signals and positive feedback effects of estrogen. Conversely, ER-expressing cells in the preoptic area project to the SCN (58), providing a mechanism for steroidal feedback to the circadian system. The stimulatory peptide kisspeptin is robustly expressed in the AVPV, with kisspeptin-ir cells expressing ERα and showing a pattern of activation consistent with a role in driving the LH surge (38, 59, 60). It remains to be established whether the SCN projects to kisspeptin cells in the AVPV or to cells of an unidentified phenotype. Furthermore, RFRP cells project extensively to the AVPV (21), suggesting potential interactions between the RFRP and kisspeptin systems in this nucleus and opportunity for further exploration (Fig. 10).

The present studies provide evidence for incorporating the RFRP system into the conceptual framework for the ovulatory machinery of some rodents and perhaps other species. These data suggest a neural route of communication from the SCN clock to an inhibitory peptidergic pathway mediating the negative feedback effects of estradiol. Additionally, the RFRP system is in a position to amalgamate with the well-established pathways and mechanisms responsible for initiating the LH surge (Fig. 10). Together, these findings suggest the possibility that the DMH and the RFRP system play a significant role in modulating the LH surge and ovulation.

Acknowledgments

We thank Drs. Irving Zucker, Eric Bittman, Ilia Karatsoreos, and Amy Hale for helpful comments and discussions on an earlier version of this paper and Connie Wang for technical support.

Received March 6, 2008. Accepted June 11, 2008.

Address all correspondence and requests for reprints to: Lance J. Kriegsfeld, Ph.D., Neurobiology Laboratory, Department of Psychology and Helen Wills Neuroscience Institute, 3210 Tolman Hall, 1650, University of California, Berkeley, California 94720-1650. E-mail: Kriegsfeld@berkeley.edu.

This work was supported by National Institutes of Health Grant HD-050470 (L.J.K.), National Science Foundation IOB-0641188 (G.E.B.), and the University of California Berkeley Committee on Research grants (L.J.K. and G.E.B.).

Disclosure Statement: The authors of this manuscript have nothing to declare.

References

1. **Stephan FK, Zucker I** 1972 Circadian rhythms in drinking behavior and locomotor activity of rats are eliminated by hypothalamic lesions. Proc Natl Acad Sci USA 69:1583–1586
2. **Moore RY, Eichler VB** 1972 Loss of a circadian adrenal corticosterone rhythm following suprachiasmatic lesions in the rat. Brain Res 42:201–206
3. **Kriegsfeld LJ, Silver R** 2006 The regulation of neuroendocrine function: timing is everything. Horm Behav 49:557–574
4. **Miller BH, Olson SL, Turek FW, Levine JE, Horton TH, Takahashi JS** 2004 Circadian clock mutation disrupts estrous cyclicity and maintenance of pregnancy. Curr Biol 14:1367–1373
5. **Nunez AA, Stephan FK** 1977 The effects of hypothalamic knife cuts on drinking rhythms and the estrus cycle of the rat. Behav Biol 20:224–234
6. **Wiegand SJ, Terasawa E** 1982 Discrete lesions reveal functional heterogeneity of suprachiasmatic structures in regulation of gonadotropin secretion in the female rat. Neuroendocrinology 34:395–404
7. **Silverman AJ, Witkin JW** 1994 Biosynthesis of gonadotropin-releasing hormone during the rat estrous cycle: a cellular analysis. Neuroendocrinology 59:545–551
8. **Herbison AE** 2006 Physiology of the GnRH neuronal network. In: Neill JD, ed. Knobil and Neill's physiology of reproduction. San Diego: Academic Press; 1415–1482
9. **de la Iglesia HO, Meyer J, Schwartz WJ** 2003 Lateralization of circadian pacemaker output: activation of left- and right-sided luteinizing hormone-releasing hormone neurons involves a neural rather than a humoral pathway. J Neurosci 23:7412–7414
10. **Petersen SL, Ottem EN, Carpenter CD** 2003 Direct and indirect regulation of gonadotropin-releasing hormone neurons by estradiol. Biol Reprod 69: 1771–1778
11. **Levine JE** 1997 New concepts of the neuroendocrine regulation of gonadotropin surges in rats. Biol Reprod 56:293–302
12. **Karsch FJ, Bowen JM, Caraty A, Evans NP, Moenter SM** 1997 Gonadotropin-releasing hormone requirements for ovulation. Biol Reprod 56:303–309
13. **Seegal RF, Goldman BD** 1975 Effects of photoperiod on cyclicity and serum gonadotropins in the Syrian hamster. Biol Reprod 12:223–231
14. **Yamaji T, Dierschke DJ, Hotchkiss J, Bhattacharya AN, Surve AH, Knobil E** 1971 Estrogen induction of LH release in the rhesus monkey. Endocrinology 89:1034–1041
15. **Karsch FJ, Weick RF, Butler WR, Dierschke DJ, Krey LC, Weiss G, Hotchkiss J, Yamaji T, Knobil E** 1973 Induced LH surges in the rhesus monkey: strength-duration characteristics of the estrogen stimulus. Endocrinology 92:1740–1747
16. **Knobil E** 1974 On the control of gonadotropin secretion in the rhesus monkey. Recent Prog Horm Res 30:1–46
17. **Legan SJ, Coon GA, Karsch FJ** 1975 Role of estrogen as initiator of daily LH surges in the ovariectomized rat. Endocrinology 96:50–56
18. **Legan SJ, Karsch FJ** 1975 A daily signal for the LH surge in the rat. Endocrinology 96:57–62
19. **Horvath TL, Cela V, van der Beek EM** 1998 Gender-specific apposition between vasoactive intestinal peptide-containing axons and gonadotrophin-releasing hormone-producing neurons in the rat. Brain Res 795:277–281
20. **van der Beek EM, Horvath TL, Wiegant VM, van den Hurk R, Buijs RM** 1997 Evidence for a direct neuronal pathway from the suprachiasmatic nucleus to the gonadotropin-releasing hormone system: combined tracing and light and electron microscopic immunocytochemical studies. J Comp Neurol 384:569–579
21. **Kriegsfeld LJ, Mei DF, Bentley GE, Ubuka T, Mason AO, Inoue K, Ukena K, Tsutsui K, Silver R** 2006 Identification and characterization of a gonadotropin-inhibitory system in the brains of mammals. Proc Natl Acad Sci USA 103:2410–2415
22. **Tsutsui K, Saigoh E, Ukena K, Teranishi H, Fujisawa Y, Kikuchi M, Ishii S, Sharp PJ** 2000 A novel avian hypothalamic peptide inhibiting gonadotropin release. Biochem Biophys Res Commun 275:661–667
23. **Osugi T, Ukena K, Bentley GE, O'Brien S, Moore IT, Wingfield JC, Tsutsui K** 2004 Gonadotropin-inhibitory hormone in Gambel's white-crowned sparrow (*Zonotrichia leucophrys gambelii*): cDNA identification, transcript localization and functional effects in laboratory and field experiments. J Endocrinol 182:33–42
24. **Ciccone NA, Dunn IC, Boswell T, Tsutsui K, Ubuka T, Ukena K, Sharp PJ** 2004 Gonadotrophin inhibitory hormone depresses gonadotrophin α and follicle-stimulating hormone β subunit expression in the pituitary of the domestic chicken. J Neuroendocrinol 16:999–1006
25. **Ubuka T, Ukena K, Sharp PJ, Bentley GE, Tsutsui K** 2006 Gonadotropin-inhibitory hormone inhibits gonadal development and maintenance by decreasing gonadotropin synthesis and release in male quail. Endocrinology 147:1187–1194
26. **Johnson MA, Tsutsui K, Fraley GS** 2007 Rat RFamide-related peptide-3 stimulates GH secretion, inhibits LH secretion, and has variable effects on sex behavior in the adult male rat. Horm Behav 51:171–180
27. **de la Iglesia HO, Meyer J, Carpino Jr A, Schwartz WJ** 2000 Antiphase oscillation of the left and right suprachiasmatic nuclei. Science 290:799–801
28. **Tavakoli-Nezhad M, Schwartz WJ** 2005 c-Fos expression in the brains of behaviorally "split" hamsters in constant light: calling attention to a dorsolateral region of the suprachiasmatic nucleus and the medial division of the lateral habenula. J Biol Rhythms 20:419–429
29. **Yan L, Foley NC, Bobula JM, Kriegsfeld LJ, Silver R** 2005 Two antiphase oscillations occur in each suprachiasmatic nucleus of behaviorally split hamsters. J Neurosci 25:9017–9026
30. **Swann JM, Turek FW** 1985 Multiple circadian oscillators regulate the timing of behavioral and endocrine rhythms in female golden hamsters. Science 228:898–900
31. **Orsini M** 1961 The external vaginal phenomena characterizing the stages of the estrous cycle, pregnancy, pseudopregnancy, lactation and anestrous hamster, *Mesocricetus auratus* Waterhouse. Proc Animal Care Panel 14:193–206
32. **Meyer-Bernstein EL, Jetton AE, Matsumoto SI, Markuns JF, Lehman MN, Bittman EL** 1999 Effects of suprachiasmatic transplants on circadian rhythms of neuroendocrine function in golden hamsters. Endocrinology 140:207–218
33. **Norman RL, Blake CA, Sawyer CH** 1973 Estrogen-dependent 24-hour periodicity in pituitary LH release in the female hamster. Endocrinology 93:965–970
34. **Bentley GE, Kriegsfeld LJ, Osugi T, Ukena K, O'Brien S, Perfito N, Moore IT, Tsutsui K, Wingfield JC** 2006 Interactions of gonadotropin-releasing hormone (GnRH) and gonadotropin-inhibitory hormone (GnIH) in birds and mammals. J Exp Zoolog A Comp Exp Biol 305:807–814
35. **Tsutsui K, Ubuka T, Yin H, Osugi T, Ukena K, Bentley GE, Ciccone N, Inoue K, Chowdhury VS, Sharp PJ, Wingfield JC** 2006 Mode of action and functional significance of avian gonadotropin-inhibitory hormone (GnIH): a review. J Exp Zoolog A Comp Exp Biol 305:801–806
36. **Tsutsui K, Bentley GE, Ubuka T, Saigoh E, Yin H, Osugi T, Inoue K, Chowdhury VS, Ukena K, Ciccone N, Sharp PJ, Wingfield JC** 2007 The general and comparative biology of gonadotropin-inhibitory hormone (GnIH). Gen Comp Endocrinol 153:365–370
37. **Hinuma S, Shintani Y, Fukusumi S, Iijima N, Matsumoto Y, Hosoya M, Fujii R, Watanabe T, Kikuchi K, Terao Y, Yano T, Yamamoto T, Kawamata Y, Habata Y, Asada M, Kitada C, Kurokawa T, Onda H, Nishimura O, Tanaka M, Ibata Y, Fujino M** 2000 New neuropeptides containing carboxy-terminal RFamide and their receptor in mammals. Nat Cell Biol 2:703–708
38. **Grieves TJ, Mason AO, Scotti MA, Levine J, Ketterson ED, Kriegsfeld LJ, Demas GE** 2007 Environmental control of kisspeptin: implications for seasonal reproduction. Endocrinology 148:1158–1166
39. **Stetson MH** 1978 Circadian organization and female reproductive cyclicity. Adv Exp Med Biol 108:251–274
40. **Hoffman GE, Lyo D** 2002 Anatomical markers of activity in neuroendocrine systems: are we all 'fos-ed out'? J Neuroendocrinol 14:259–268
41. **Adler BA, Crowley WR** 1986 Evidence for γ-aminobutyric acid modulation of ovarian hormonal effects on luteinizing hormone secretion and hypothalamic catecholamine activity in the female rat. Endocrinology 118:91–97
42. **Demling J, Fuchs E, Baumert M, Wuttke W** 1985 Preoptic catecholamine, GABA, and glutamate release in ovariectomized and ovariectomized estrogen-primed rats utilizing a push-pull cannula technique. Neuroendocrinology 41:212–218
43. **Hartman RD, He JR, Barraclough CA** 1990 γ-Aminobutyric acid-A and -B receptor antagonists increase luteinizing hormone-releasing hormone neuronal responsiveness to intracerebroventricular norepinephrine in ovariectomized estrogen-treated rats. Endocrinology 127:1336–1345
44. **Kumru S, Simsek M, Yilmaz B, Sapmaz E, Kutlu S, Sandal S, Canpolat S** 2001 Differential regulation of preovulatory luteinizing hormone and follicle-stimulating hormone release by opioids in the proestrous rat. Physiol Res 50:397–403
45. **Gopalan C, Gilmore DP, Brown CH** 1989 Effects of different opiates on hypothalamic monoamine turnover and on plasma LH levels in pro-oestrous rats. J Neurol Sci 94:211–219
46. **Barkan A, Regiani S, Duncan J, Papavasiliou S, Marshall JC** 1983 Opioids modulate pituitary receptors for gonadotropin-releasing hormone. Endocrinology 112:387–389
47. **Berriman SJ, Wade GN, Blaustein JD** 1992 Expression of Fos-like proteins in gonadotropin-releasing hormone neurons of Syrian hamsters: effects of estrous cycles and metabolic fuels. Endocrinology 131:2222–2228
48. **Wang HJ, Hoffman GE, Smith MS** 1995 Increased GnRH mRNA in the GnRH neurons expressing cFos during the proestrous LH surge. Endocrinology 136: 3673–3676
49. **Hoffman GE, Smith MS, Verbalis JG** 1993 c-Fos and related immediate early gene products as markers of activity in neuroendocrine systems. Front Neuroendocrinol 14:173–213
50. **Lee WS, Abbud R, Smith MS, Hoffman GE** 1992 LHRH neurons express cJun protein during the proestrous surge of luteinizing hormone. Endocrinology 130:3101–3103
51. **Lee WS, Smith MS, Hoffman GE** 1990 Luteinizing hormone-releasing hormone neurons express Fos protein during the proestrous surge of luteinizing hormone. Proc Natl Acad Sci USA 87:5163–5167
52. **Kriegsfeld LJ** 2006 Driving reproduction: RFamide peptides behind the wheel. Horm Behav 50:655–666
53. **Anderson G, Rizwan, MZ** RFRP-3 inhibits GnRH neuronal activation during

the estradiol-induced LH surge. Proc 37th Annual Meeting of Society for Neuroscience, San Diego, CA, 2007 (Abstract 556.7)
54. **Silver R, LeSauter J, Tresco PA, Lehman MN** 1996 A diffusible coupling signal from the transplanted suprachiasmatic nucleus controlling circadian locomotor rhythms. Nature 382:810–813
55. **Hakim H, DeBernardo AP, Silver R** 1991 Circadian locomotor rhythms, but not photoperiodic responses, survive surgical isolation of the SCN in hamsters. J Biol Rhythms 6:97–113
56. **Le WW, Attardi B, Berghorn KA, Blaustein J, Hoffman GE** 1997 Progesterone blockade of a luteinizing hormone surge blocks luteinizing hormone-releasing hormone Fos activation and activation of its preoptic area afferents. Brain Res 778:272–280
57. **Watson Jr RE, Langub Jr MC, Engle MG, Maley BE** 1995 Estrogen-receptive neurons in the anteroventral periventricular nucleus are synaptic targets of the suprachiasmatic nucleus and peri-suprachiasmatic region. Brain Res 689:254–264
58. **de la Iglesia HO, Blaustein JD, Bittman EL** 1999 Oestrogen receptor-α-immunoreactive neurones project to the suprachiasmatic nucleus of the female Syrian hamster. J Neuroendocrinol 11:481–490
59. **Smith JT, Popa SM, Clifton DK, Hoffman GE, Steiner RA** 2006 Kiss1 neurons in the forebrain as central processors for generating the preovulatory luteinizing hormone surge. J Neurosci 26:6687–6694
60. **Adachi S, Yamada S, Takatsu Y, Matsui H, Kinoshita M, Takase K, Sugiura H, Ohtaki T, Matsumoto H, Uenoyama Y, Tsukamura H, Inoue K, Maeda K** 2007 Involvement of anteroventral periventricular metastin/kisspeptin neurons in estrogen positive feedback action on luteinizing hormone release in female rats. J Reprod Dev 53:367–378
61. **de la Iglesia HO, Blaustein JD, Bittman EL** 1995 The suprachiasmatic area in the female hamster projects to neurons containing estrogen receptors and GnRH. Neuroreport 6:1715–1722
62. **Irwig MS, Fraley GS, Smith JT, Acohido BV, Popa SM, Cunningham MJ, Gottsch ML, Clifton DK, Steiner RA** 2004 Kisspeptin activation of gonadotropin releasing hormone neurons and regulation of KiSS-1 mRNA in the male rat. Neuroendocrinology 80:264–272
63. **Kauffman AS, Clifton DK, Steiner RA** 2007 Emerging ideas about kisspeptin-GPR54 signaling in the neuroendocrine regulation of reproduction. Trends Neurosci 30:504–511
64. **Simonian SX, Spratt DP, Herbison AE** 1999 Identification and characterization of estrogen receptor α-containing neurons projecting to the vicinity of the gonadotropin-releasing hormone perikarya in the rostral preoptic area of the rat. J Comp Neurol 411:346–358
65. **Ubuka T, Kim S, Huang Y, Reid J, Jiang J, Osugi T, Chowdhury VS, Tsutsui K, Bentley GE** 2008 Gonadotropin-inhibitory hormone neurons interact directly with gonadotropin-releasing hormone-I and -II neurons in European starling brain. Endocrinology 149:268–278.

***Endocrinology* is published monthly by The Endocrine Society (http://www.endo-society.org), the foremost professional society serving the endocrine community.**